Vascular Smooth Muscle ROCK1 Contributes to Hypoxia-Induced Pulmonary Hypertension Development in Mice

Krishna C. Penumatsa[1], **Adit A. Singhal**[1], **Rod R. Warburton**[1], **Michael D. Bear**[1,Θ], **Chinmayee D. Bhedi**[1], **Sabina Nasirova**[1], **Jamie L. Wilson**[1], **Guanming Qi**[1], **Ioana R. Preston**[1], **Nicholas S. Hill**[1], **Barry L. Fanburg**[1], **Young-Bum Kim**[2], **Deniz Toksoz**[1,#]

[1]Division of Pulmonary, Critical Care and Sleep, Tufts Medical Center, 800 Washington St., Boston, MA 02111

[2]Division of Endocrinology, Diabetes and Metabolism, Beth Israel Deaconess Medical Center, 330 Brookline Ave., Boston, MA 02115

Abstract

Rho kinase (ROCK) is implicated in the development of pulmonary arterial hypertension (PAH) in which abnormal pulmonary vascular smooth muscle (VSM) contractility and remodeling lead to right heart failure. Pharmacologic ROCK inhibitors block experimental pulmonary hypertension (PH) development in rodents but can have off-target effects and do not distinguish between the two ROCK forms, ROCK1 and ROCK2, encoded by separate genes. An earlier study using gene knock out (KO) in mice indicated that VSM ROCK2 is required for experimental PH development, but the role of ROCK1 is not well understood. Here we investigated the in vivo role of ROCK1 in PH development by generating a VSM-targeted homozygous ROCK1 gene KO mouse strain. Adult control mice exposed to Sugen5416 (Su)/hypoxia treatment to induce PH had significantly increased right ventricular systolic pressures (RVSP) and RV hypertrophy versus normoxic controls. In contrast, Su/hypoxia-exposed VSM ROCK1 KO mice did not exhibit significant RVSP elevation, and RV hypertrophy was blunted. Su/hypoxia-induced pulmonary small vessel muscularization was similarly elevated in both control and VSM ROCK1 KO animals. siRNA-mediated ROCK1 knock-down (KD) in human PAH pulmonary arterial SM cells (PASMC) did not affect cell growth. However, ROCK1 KD led to reduced AKT and MYPT1 signaling in serotonin-treated PAH PASMC. The findings suggest that like VSM ROCK2, VSM ROCK1 actively contributes to PH development, but in distinction acts via nonproliferative pathways to promote hypoxemia, and thus may be a distinct therapeutic target in PH.

[#]Corresponding author: Deniz Toksoz, Ph.D., Division of Pulmonary, Critical Care and Sleep, Tufts Medical Center, Tufts University School of Medicine, Boston, MA 02111; Tel: 617 636 1041 : dtoksoz@tuftsmedicalcenter.org.
[Θ]Current address: Dept. of Pharmacy Practice, MCPHS University, Worcester, MA 01608

Declaration of competing interest: The authors declare that they have no conflicts of interest.

1. INTRODUCTION

Pulmonary hypertension (PH) is defined by high pressure in the pulmonary arteries of patients resulting in exertional shortness of breath and hypoxemia leading to heart failure [1]. Group 1 PH, also known as pulmonary arterial hypertension (PAH), is a PH subtype whose pathogenesis involves obstructive vascular remodeling and sustained/ elevated pulmonary vascular contractility, culminating in right heart failure [1]. Despite the availability of several therapeutic agents, none effectively halt PAH progression, and there is a need to define new therapeutic targets.

Studies have shown that the serine/threonine kinase, Rho kinase (ROCK), mediates a broad range of cellular responses thought to be involved in PAH such as pulmonary vascular smooth muscle (VSM) cell contractility and mitogenesis, among others [2]. ROCK mediates Ca^{2+} sensitization of VSM cell contractility by phosphorylating and thus inhibiting the myosin phosphatase target subunit 1 (MYPT1) of protein phosphatase1, resulting in acto-myosin filament-mediated cell contraction [2]. The commonly available pharmacologic ROCK inhibitors (Y2763; fasudil *aka* HA1077) have been extensively used both in vitro and in animal models of experimental PH to block responses associated with PH [3]. Moreover, use of these inhibitors in clinical studies have yielded findings supportive of ROCK as a therapeutic target for PAH [3]. However, ROCK inhibitor-based studies have limitations due to off-target effects on related kinases [4], particularly when used at higher levels in vivo.

ROCK is encoded by two genes that generate ROCK1 (*aka* p160ROCK, ROKβ) and ROCK2 (*aka* ROKα) kinases; both ROCK1 and ROCK2 contain highly similar catalytic domains, yet otherwise encode divergent protein sequence [2]. Since the commonly available ROCK inhibitors do not distinguish between the two ROCK forms [2], this has impeded a clear understanding of the in vivo roles of ROCK isoforms in disease. Use of genetically altered mouse models provides an alternative approach to analyzing ROCK roles in vivo, including in PH development. With this approach, VSM tissue-targeted ROCK2 haplo-insufficient mice were shown to be protected from hypoxia-induced PH development [5], validating a contributory role for ROCK2 in PH.

However, there has been limited knowledge on the in vivo role of ROCK1 in PH development. In the present study we pursued a genetic approach to address this by generating a VSM-targeted ROCK1 homozygous KO (termed VSM ROCK1 KO) mouse strain, and analyzing its responses to chronic hypoxia exposure, as well as examining the role of ROCK1 in PAH patient-derived PASMC.

2. MATERIALS AND METHODS

2.1 Reagents:

SUGEN-5416 (Su) was from Tocris Bioscience (Bristol, UK). Serotonin and recombinant human PDGF-BB were from Sigma (St. Louis, MO).

2.2 Mouse strains:

To generate the SM22Cre:ROCK1 KO line, the loxP site-flanked ("floxed") ROCK1 gene mouse strain that we previously generated [6] was bred with the SM22αCre mouse strain (ww/Cre+) (JAXLAB, Bar Harbor, ME) that contains Cre recombinase gene whose expression is driven by the VSM-targeted SM22α promoter [7].

2.3 Genotyping:

Floxed ROCK1 alleles were identified by mouse DNA PCR using the primer pair: 5'-CCTGATGAGCAACTATGACGTGCC-3' and 5'-GTACAGTACAGGAGCTACAAAATTAG-3'. Amplification products are 320 and 380 base pairs for the wild-type (WT) and floxxed ROCK1 alleles, respectively [6]. The SM22αCre allele was detected by PCR of universal Cre recombinase primer sequences. PCR was carried out using the Taq PCR Kit (New England Biolabs, Ipswich, MA). PCR products were resolved on 2.2% agarose gels using the FlashGel System (Lonza, Rockland, ME).

2.4 Induction of experimental pulmonary hypertension in mice:

All animal studies were approved by the Tufts Institutional Animal Care Commitee. PH was experimentally induced in male mice (16 – 20 weeks) using the Sugen/hypoxia (Su/hypoxia) model [8]. For hypoxic exposure, mice were placed in normobaric hypoxic (FIO_2 10.5%) chambers (Biospherix, Parish, NY) for 4 weeks. Sugen 5416 was given weekly to hypoxia-exposed mice as previously reported [9] (Sugen 5416 does not induce PH on its own). Room air-exposed littermates constituted normoxia controls and were given equal volume of vehicle.

2.5 Hemodynamic measurements:

Before and after Su/hypoxia exposure, systemic pressures were measured using a non-invasive tail cuff pressure system (ADInstruments, PowerLab NIBP Controller, Colorado Springs, CO). Body weights were recorded. Right ventricular systolic pressures were measured as previoiusly described [9]. The heart was removed and the right ventricle (RV) was separated from the left ventricle (LV) and septum (S). Ventricle weights were recorded.

2.6 Lung histology:

To assess vessel muscularization, paraffin-embedded lung sections were stained with Verhoeff-VanGieson for elastin, a VSM marker. 50 intra-acinar arteries (20–80 μm diameter) were scored for muscularization by a treatment-blind investigator using light microscopy (Zeiss, Thornwood, NY).

2.7 Antibodies:

Antibodies to phospho-Akt (p-AKT Ser473), AKT, and HRP-conjugated mouse and rabbit secondary antibodies were from Cell Signaling Technology (Beverly, MA). Anti-phospho-MYPT1 (p-MYPT1 Th696) rabbit polyclonal antibody was from ThermoFisher (NY). Antibodies to MYPT1, ROCK1, ROCK2, smooth muscle actin (SMA) and GAPDH were from Santa Cruz Biotechnology (San Diego, CA).

2.8 Immunoblotting:

Cell lysates were immunoblotted and immunoreactive bands were detected as reported [10]. Quantification of band intensity was performed by densitometry using ProteinSimple software, and phospho-protein levels were normalized to corresponding total protein values that were initially normalized to corresponding GAPDH or actin values.

2.9 Cell culture:

Human PASMCs isolated from pulmonary arteries of idiopathic PAH patients (PAHPASMC; gift) were grown as described [11] and used at passages 5–8.

2.10 siRNA transfection:

19mer ready-to-use validated human ROCK1 siRNA (ON-TARGET Plus, Dharmacon, Lafayette, CO) and negative control Silencer siRNA (ThermoFisher Scientific) were transfected into cells at a final concentration of 50 nM using Lipofectamine 2000 (ThermoFisher Scientific) as recommended by the manufacturer.

2.11 Cell growth:

Cell viability as a measure of growth was measured in 96-well plates using the CellTiter-Glo Luminescent Cell Viability Assay (Promega, Madison, WI). Data was recorded by luminometer.

2.12 Statistical analysis:

Data are presented as mean $\pm$ SEM in bar graphs, or mean $\pm$ range in box plots, unless otherwise noted. Statistical analysis was performed using Student's *t-test* for two experimental groups, or ANOVA for multiple groups using Tukeys multiple comparison test; differences were considered significant where $p<0.05$.

3. RESULTS

3.1 SM22Cre:ROCK1 KO mouse strain is viable and exhibits normal physiology compared to controls.

Animals containing the floxed ROCK1 allele were bred with the SM22αCre line to obtain heterozygous floxed ROCK1/Cre+ animals, and these were cross-bred. As determined by PCR genotyping (Figure 1A), this breeding strategy generated the SM22Cre:ROCK1 KO strain (cc/+) from here on referred to as VSM ROCK1 KO, that is homozygous for the floxed ROCK1 alelle (cc; top panel) and contains the SM22Cre allele (+, bottom panel). To avoid genetic drift, homozygous cc VSM ROCK1 KO were generated from heterozygous crosses for use in experiments. Cre-negative mice generated from these breedings constituted WT littermate controls.

The Mendelian ratios of offspring from crosses of heterozygous KO mice were as expected, indicating that VSM ROCK1 KO embryos are viable; furthermore these VSM ROCK1 KO animals grew normally to adulthood. In normoxia, there was no significant difference in body weights or systemic blood pressures between WT and VSM ROCK1 KO animals (Fig

1B and Fig 1C). Animals were next exposed to Su/hypoxia for 4 weeks; at the end of the exposure there was no significant difference in body weights and systolic pressures (Fig 1B and 1C) between the two groups.

3.2 VSM ROCK1 KO mice display a blunted pulmonary vascular pressure response to Su/hypoxia.

We next investigated the effect of Su/hypoxia treatment on a major endpoint of PH development: increased right ventricular systolic pressure (RVSP) [1]. In normoxia, WT and VSM ROCK1 KO mice displayed comparable mean RVSP mean values (Figure 1D; WT: 24.4 vs. KO: 23.7; p=0.9). Following Su/hypoxia treatment, as expected, WT mice had significantly elevated mean RVSP values compared to normoxic WT counterparts (34.4 vs. 24.4; p<0.0001) (Figure 1D). In contrast, there was no significant difference in mean RVSP values of Su/hypoxic VSM ROCK1 KO mice compared to normoxic KO mice (26.9 vs. 23.7; p=0.15), or to normoxic WT mice (26.9 vs. 24.4; p=0.37). Also, mean RVSP values for Su/hypoxic VSM ROCK1 KO mice were significantly lower than for Su/hypoxic WT mice (KO: 26.9 vs WT: 34.4; p=0.0003).

3.3 VSM ROCK1 KO mice display a reduced RV hypertrophic response to Su/hypoxia.

Another key endpoint of PAH is a cardiac hypertrophic response restricted to the right ventricle (RV) [1] as measured by determining the Fulton index (RV/LV+S mass ratio) (the left ventricle and septum (LV+S) is largely unaffected). As expected, the mean Fulton index value of Su/hypoxic WT mice was significantly increased compared to normoxic WT counterparts (0.30 vs. 0.24; p=0.0002) (Figure 1E). In contrast, the mean Fulton index value of Su/hypoxic VSM ROCK1 KO mice (0.27) was not significantly different from either normoxic VSM ROCK1 KO (0.25) or normoxic WT control values (0.24). Moreover, the mean Fulton index value of Su/hypoxic KO mice was lower compared to the Su/hypoxic WT value (0.27 vs. 0.30), and approached significance (p=0.08).

A related index of RV hypertrophy is the RV mass/body weight ratio (RV/BW) which paralleled the Fulton index values of the two groups (Figure 1F). As expected, mean Su/hypoxic WT RV/BW values were significantly increased compared to normoxic WT values (1.12 vs. 0.76; p=0.0007). In contrast, Su/hypoxic VSM ROCK1 KO RV/BW values were not significantly different from normoxic VSM ROCK1 KO values (0.92 vs. 0.77; p=0.24), and were lower than Su/hypoxic WT values (1.12), although this didn't reach significance (p=0.1). As expected, there was no significant difference in left ventricular (LV)/body mass ratios (LV/BW; Figure 1G) between any groups (mean WT Su/hypoxic value 3.6 vs. WT normoxic 3.2, p=0.4; mean VSM ROCK1 KO Su/hypoxic value 3.3 vs KO normoxic 3.2, p=0.90).

3.4 WT and VSM ROCK1 KO mice exhibit comparable increased pulmonary small vessel neomuscularization in response to Su/hypoxia.

Chronic hypoxia induces remodeling of distal small (50–80 nm) pulmonary vessels that become neomuscularized [12]. To examine this, 50 intra-acinar arteries from elastin-stained lung sections (n=4 mice per group) were blind-scored into fully muscular (>75% of

the circumference of the vessel), partially muscular (25–75%), or nonmuscular (<25%) categories.

In normoxia, as expected the majority of small vessels in both WT and VSM ROCK1 KO groups were scored as non-muscularized (Figure 2A and 2B), with no significant difference between them. Furthermore, there were no differences in the percentages of partial- and full-muscularized categories between the two groups. As expected, Su/hypoxia exposure led to significant increases in WT lungs of the partial- and full-muscularized categories (Figure 2C and 2D); comparable increases in muscularized small vessels were also detected in Su/hypoxic VSM ROCK1 KO animals (Figure 2D) in those categories, with no significant differences between WT and KO groups within each category.

3.5 ROCK1 knock-down in human PAH PASMC does not alter cell growth.

To further examine the role of ROCK1 in PH, we used cultured human idiopathic PAH PASMC which represent a more relevant cell type to the human disease than mouse cells (VSM cells from WT and KO mice pulmonary artery tissue failed to grow sufficiently). Given the lack of effect of ROCK1 KO on Su/hypoxia-induced small vessel muscularization (Figure 2), we investigated the role of ROCK1 in PAH PASMC growth using siRNA-mediated knock-down (KD). Cells transfected with scrambled (scr) control or human ROCK1 siRNA were transferred to low-serum media overnight. Cells were then stimulated with two growth factors implicated in PAH pathogenesis: PDGF which is a strong mitogen for WT PASMC [13], and the vasoconstrictor serotonin (5-HT) which is also a modest mitogen for WT PASMC [14]. After 48 hours, PDGF treatment led to robust cell growth in the si-scr group; ROCK1 KD had no effect on PDGF-induced growth (Figure 3A). 5-HT treatment led to a minor increase in cell growth in the si-scr group (below significance, p=0.07), and ROCK1 KD had no effect on this (Figure 3A). Immunoblotting verified si-RNA-mediated ROCK1 KD by ~50% (Figure 3B).

3.6 ROCK1 mediates 5-HT signaling in human PAH PASMC.

We next evaluated the role of ROCK1 in the AKT and ROCK signaling pathways thought to contribute to PAH pathogenesis [15, 16] using the same stimuli. PAH PASMC transfected with scr control or human ROCK1 siRNA were transferred to low-serum media overnight, and 48 hours later briefly stimulated with PDGF followed by lysis. Immunoblotting vehicle-stimulated cell lysates for activated p-AKT (Ser473) showed no difference between the scr and ROCK1 siRNA groups (Figure 4A and 4B). PDGF stimulation led to a robust induction of p-AKT levels in the scr group that was not affected by si-ROCK1 (Figure 4A and 4B). There was no significant change in p-MYPT1 levels upon PDGF stimulation, and no effect by si-ROCK1 KD. Immunoblotting confirmed significant ROCK1 KD by si-ROCK1, while ROCK2 levels were unchanged (Figures 4A and 4B).

Parallel experiments using 5-HT as the stimulus showed a modest but significant ~1.4-fold increase in p-AKT levels in the si-scr group which was strongly inhibited by si-ROCK1 (Figure 4C and 4D). 5-HT stimulation did not lead to an increase in p-MYPT1 levels in the si-scr group; however, the combination of 5-HT with si-ROCK1 led to a significant ~50% reduction in p-MYPT1 levels (Figure 4C and 4D). Immunoblotting of transfected

cells verified ROCK1 KD, with ROCK2 levels unchanged (Figures 4C and 4D), and no off-target effect of ROCK1 si-RNA on GAPDH levels.

4. DISCUSSION

The finding of overall normal development of SM22Cre:ROCK1 KO pups indicates that VSM ROCK1 is not required for normal embryonic development, at least after developmental stage E10.5 which is when SM22α becomes expressed [7]. The normal systemic pressures of adult VSM ROCK1 KO animals under normoxia and Su/hypoxia (Figure 1B) suggest that selective ROCK1 inhibition may potentially avoid hypotension side-effects. While the elevated RVSP response of WT littermates in response to Su/hypoxia was significant (Figure 1C), the magnitude of the response was not as large as in other reports using the more common C57/Bl6 mouse strain. Mouse strain differences can influence RVSP responses to hypoxia [17], and the C57Bl6/SJL hybrid gene background of the strain generated here is a likely factor affecting the magnitude.

The significantly blunted RVSP response of the VSM ROCK1 KO strain to Su/hypoxia compared to WT (Figure 1C) demonstrates for the first time that VSM ROCK1 plays a significant role in hypoxia-induced PH development that is separate from that of VSM ROCK2. The finding that VSM ROCK1 does not play a major role in Su/hypoxia-induced small vessel muscularization (Figure 2) is in distinction to VSM ROCK2 [5]. There are some limitations to this morphometric analysis method, since the visual scoring method is of limited sensitivity. In either case, the precise contribution of microvasculature structural changes in PH remains partially understood [18]. Moreover, the morphometry does not measure vessel functionality and hence effects of ROCK1 KO on small vessel function such as contractility cannot be ruled out; such a functional role for ROCK1 is supported by our previous work showing that ROCK1 contributes to the contractile response of human PASMC to endothelin-1 [19]. ROCK1 is a hypoxia-responsive gene [20]; thus, diminished ROCK1-mediated pulmonary vascular contractility is likely to be a major factor in the blunted RVSP values of Su/hypoxic VSM ROCK1 KO mice.

The reduced RVSP of Su/hypoxic VSM ROCK1 KO mice is in turn a likely major factor in the blunted Fulton index of these mice. Hypoxia-induced RV hypertrophy is a complex response involving multiple genes and pathways [21], and the partial reduction of the Fulton index of Su/hypoxic VSM ROCK1 KO animals compared to Su/hypoxic WT animals may be due to compensation by other genes, such as ROCK2.

Our finding that ROCK1 KD had no effect on baseline or PDGF-stimulated PAH PASMC growth (Figure 3) is consistent with our in vivo finding that VSM ROCK1 KO had no effect on vessel neomuscularization, the latter which involves proliferation [12]; this differs from the active role of ROCK2 in cell proliferation [5].

The lack of effect of ROCK1 KD on PDGF-induced signaling (Figure 4) further supports the conclusion that VSM ROCK1 is unlikely to play a role in proliferative pathways, in contrast to VSM ROCK2 [5]. 5-HT activates several signaling pathways in WT PASMC including AKT and ROCK [22, 23]; however its effect on human PAH PASMC signaling has not been

previously studied to our knowledge. The observed induction of p-AKT activation by 5-HT in si-scr-transfected PAH PASMC (Figure 4) is consistent with previous findings in WT PASMC [22]; the observed inhibition of 5-HT-induced p-AKT activation by ROCK1 KD suggests a novel AKT/ROCK1 cross-talk in these cells involving a nonproliferative AKT function. In contrast to our previous findings in WT PASMC [23], 5-HT did not further stimulate p-MYPT1 levels in si-scr-transfected PAH PASMC, possibly reflecting already elevated levels in these cells as described in PAH [24]. The finding that ROCK1 KD led to blunted p-MYPT1 levels in 5-HT-treated PAH PASMC suggests a role for ROCK1 in modulating p-MYPT1 in PAH cells in the context of acute stress such as 5-HT, possibly via effects on p-MYPT1 stability or subcellular localization, Overall the findings indicate a dysregulated ROCK1-MYPT1 pathway in PAH cells concordant with other reports [24, 25]. Potential limitations to these in vitro studies are that the ROCK1 KD is partial (as previously reported, likely reflecting ROCK1 protein stability [19]), and that proliferation was only assayed after 48 hours due to transient siRNA effect. Nevertheless, taken together the in vitro studies indicate a role for ROCK1 in pathways other than proliferation in PAH PASMC.

Overall, the findings demonstrate that like VSM ROCK2 [5], VSM ROCK1 participates separately in PH development in the mouse, and non-overlapping in vivo roles for ROCK1/2 have also been found in other disease models [16, 26, 27]. A limitation to our study is that the applicability of the hypoxia-induced PH model to the human disease has not been fully established; however, a strength of our study is that the in vitro results, obtained in a clinically relevant culture system (PAH PASMC), are concordant with the in vivo results. A ROCK2-selective inhibitor is currently in several clinical trials [16], while development of a ROCK1-selective inhibitor has lagged. The present findings suggest that ROCK1 inhibition may be beneficial in the setting of hypoxemia in PH. Overall, our study supports the further elucidation of ROCK1 and ROCK2 functions, and the development of selective ROCK inhibitors as potential novel therapeutic agents in PH and related pulmonary diseases.

Acknowledgments:

Funding:

REFERENCES

1. Thenappan T, et al. , Pulmonary arterial hypertension: pathogenesis and clinical management. BMJ, 2018. 360: p. j5492. [PubMed: 29540357]

2. Julian L and Olson MF, Rho-associated coiled-coil containing kinases (ROCK): structure, regulation, and functions. Small GTPases, 2014. 5: p. e29846. [PubMed: 25010901]

3. Barman SA, Zhu S, and White RE, RhoA/Rho-kinase signaling: a therapeutic target in pulmonary hypertension. Vasc Health Risk Manag, 2009. 5: p. 663–71. [PubMed: 19707285]

4. Davies SP, et al. , Specificity and mechanism of action of some commonly used protein kinase inhibitors. Biochem J, 2000. 351(Pt 1): p. 95–105. [PubMed: 10998351]

5. Shimizu T, et al. , Crucial role of ROCK2 in vascular smooth muscle cells for hypoxia-induced pulmonary hypertension in mice. Arterioscler Thromb Vasc Biol, 2013. 33(12): p. 2780–91. [PubMed: 24135024]

6. Lee DH, et al. , Targeted disruption of ROCK1 causes insulin resistance in vivo. J Biol Chem, 2009. 284(18): p. 11776–80. [PubMed: 19276091]

7. Moessler H, et al. , The SM 22 promoter directs tissue-specific expression in arterial but not in venous or visceral smooth muscle cells in transgenic mice. Development, 1996. 122(8): p. 2415–25. [PubMed: 8756287]

8. Ciuclan L, et al. , A novel murine model of severe pulmonary arterial hypertension. Am J Respir Crit Care Med, 2011. 184(10): p. 1171–82. [PubMed: 21868504]

9. Menon DP, et al. , Vascular cell-specific roles of mineralocorticoid receptors in pulmonary hypertension. Pulm Circ, 2021. 11(3): p. 20458940211025240. [PubMed: 34211700]

10. Penumatsa K, et al. , Tissue transglutaminase promotes serotonin-induced AKT signaling and mitogenesis in pulmonary vascular smooth muscle cells. Cell Signal, 2014. 26(12): p. 2818–25. [PubMed: 25218191]

11. Comhair SA, et al. , Human primary lung endothelial cells in culture. Am J Respir Cell Mol Biol, 2012. 46(6): p. 723–30. [PubMed: 22427538]

12. Stenmark KR, et al. , Dynamic and diverse changes in the functional properties of vascular smooth muscle cells in pulmonary hypertension. Cardiovasc Res, 2018. 114(4): p. 551–564. [PubMed: 29385432]

13. Barst RJ, PDGF signaling in pulmonary arterial hypertension. J Clin Invest, 2005. 115(10): p. 2691–4. [PubMed: 16200204]

14. Humbert M, et al. , Cellular and molecular pathobiology of pulmonary arterial hypertension. J Am Coll Cardiol, 2004. 43(12 Suppl S): p. 13S–24S. [PubMed: 15194174]

15. Babicheva A, Makino A, and Yuan JX, mTOR Signaling in Pulmonary Vascular Disease: Pathogenic Role and Therapeutic Target. Int J Mol Sci, 2021. 22(4).

16. Loirand G, Rho Kinases in Health and Disease: From Basic Science to Translational Research. Pharmacol Rev, 2015. 67(4): p. 1074–95. [PubMed: 26419448]

17. Jiang B, et al. , Marked Strain-Specific Differences in the SU5416 Rat Model of Severe Pulmonary Arterial Hypertension. Am J Respir Cell Mol Biol, 2016. 54(4): p. 461–8. [PubMed: 26291195]

18. Stenmark KR and McMurtry IF, Vascular remodeling versus vasoconstriction in chronic hypoxic pulmonary hypertension: a time for reappraisal? Circ Res, 2005. 97(2): p. 95–8. [PubMed: 16037575]

19. Wilson JL, et al. , Unraveling endothelin-1 induced hypercontractility of human pulmonary artery smooth muscle cells from patients with pulmonary arterial hypertension. PLoS One, 2018. 13(4): p. e0195780. [PubMed: 29649319]

20. Gilkes DM, et al. , Hypoxia-inducible factors mediate coordinated RhoA-ROCK1 expression and signaling in breast cancer cells. Proc Natl Acad Sci U S A, 2014. 111(3): p. E384–93. [PubMed: 24324133]

21. Bogaard HJ, et al. , The right ventricle under pressure: cellular and molecular mechanisms of right-heart failure in pulmonary hypertension. Chest, 2009. 135(3): p. 794–804. [PubMed: 19265089]

22. Liu Y and Fanburg BL, Serotonin-induced growth of pulmonary artery smooth muscle requires activation of phosphatidylinositol 3-kinase/serine-threonine protein kinase B/mammalian target of rapamycin/p70 ribosomal S6 kinase 1. Am J Respir Cell Mol Biol, 2006. 34(2): p. 182–91. [PubMed: 16195541]

23. Liu Y, et al. , Rho kinase-induced nuclear translocation of ERK1/ERK2 in smooth muscle cell mitogenesis caused by serotonin. Circ Res, 2004. 95(6): p. 579–86. [PubMed: 15297378]

24. Guilluy C, et al. , RhoA and Rho kinase activation in human pulmonary hypertension: role of 5-HT signaling. Am J Respir Crit Care Med, 2009. 179(12): p. 1151–8. [PubMed: 19299501]

25. Do e Z, et al. , Evidence for Rho-kinase activation in patients with pulmonary arterial hypertension. Circ J, 2009. 73(9): p. 1731–9. [PubMed: 19590140]

26. Knipe RS, et al. , The Rho Kinase Isoforms ROCK1 and ROCK2 Each Contribute to the Development of Experimental Pulmonary Fibrosis. Am J Respir Cell Mol Biol, 2018. 58(4): p. 471–481. [PubMed: 29211497]

27. Sunamura S, et al. , Different roles of myocardial ROCK1 and ROCK2 in cardiac dysfunction and postcapillary pulmonary hypertension in mice. Proc Natl Acad Sci U S A, 2018. 115(30): p. E7129–E7138. [PubMed: 29987023]

Highlights

- The Rho kinase ROCK is implicated in pulmonary hypertension (PH) development, but the role of the two ROCK forms ROCK1 and ROCK2 is partially understood.

- We investigated the role of ROCK1 in PH development by generating a vascular smooth muscle (VSM) targeted-ROCK1 gene knock-out (KO) mouse strain (VSM ROCK1 KO).

- In contrast to controls, VSM ROCK1 KO mice were protected from hypoxia-induced PH development, indicating that ROCK1 promotes PH development separately to ROCK2.
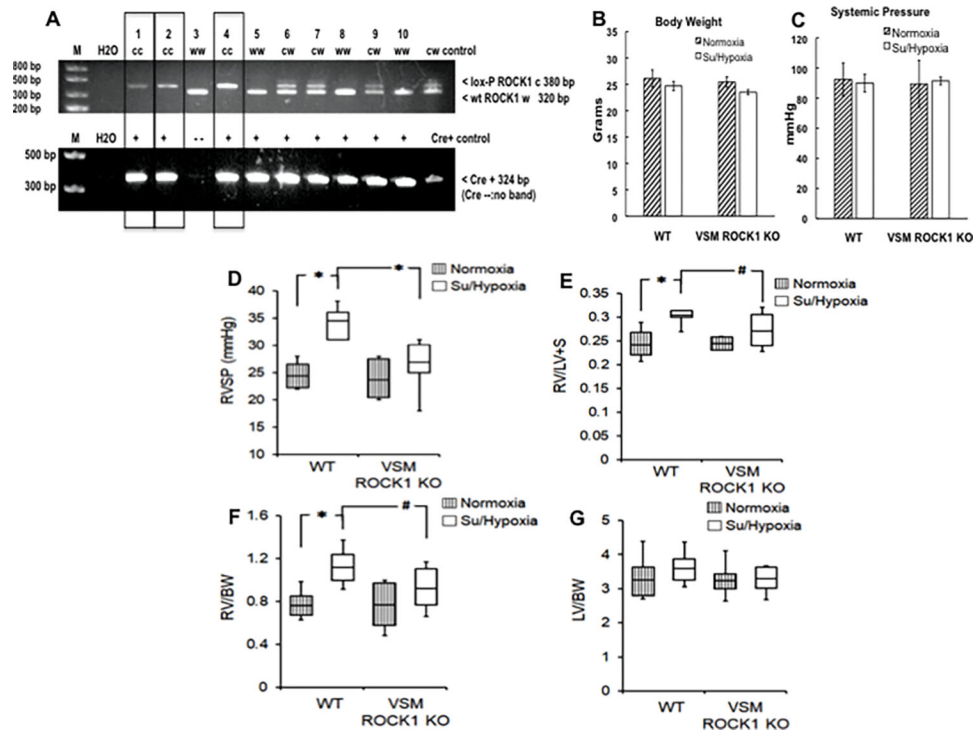
Figure 1. SM22Cre:loxP ROCK1 homozygous KO genetic validation, and response to Su/Hypoxia-induced PH development.

A) PCR analysis of DNAs 1, 2 and 4 (boxed) showing loxP ROCK1 gene homozygosity (cc) and SM22Cre allele presence (+). B) Body weights of male VSM ROCK1 KO mice and WT littermates in normoxia or after Su/Hypoxia exposure. C) Systemic pressures of VSM ROCK1 KO mice and WT littermates in normoxia or after 4 wk Su/Hypoxia exposure. D) *p<0.05 for mean right ventricular systolic pressure (RVSP) values of WT Su/hypoxic vs. normoxic littermates. *p<0.05 for mean RVSP values of Su/hypoxic VSM ROCK1 KO mice vs. Su/hypoxic WT littermates. E) *p<0.05 for mean Fulton index (RV/LV+S) values of WT Su/hypoxic vs. normoxic littermates. #p=0.08 for mean RV/LV+S values of Su/hypoxic VSM ROCK1 KO vs. Su/hypoxic WT littermates. F) *p<0.05 for mean right ventricle mass/ body weight (RV/BW) values of WT Su/hypoxic vs. normoxic WT littermates. #p=0.1 for mean RV/BW values of Su/hypoxic VSM ROCK1 KO vs. Su/hypoxic WT littermates. G) Left ventricle mass/ body weight (LV/BW) values. Box plot data represent mean + range, n = 7–9 mice / group.
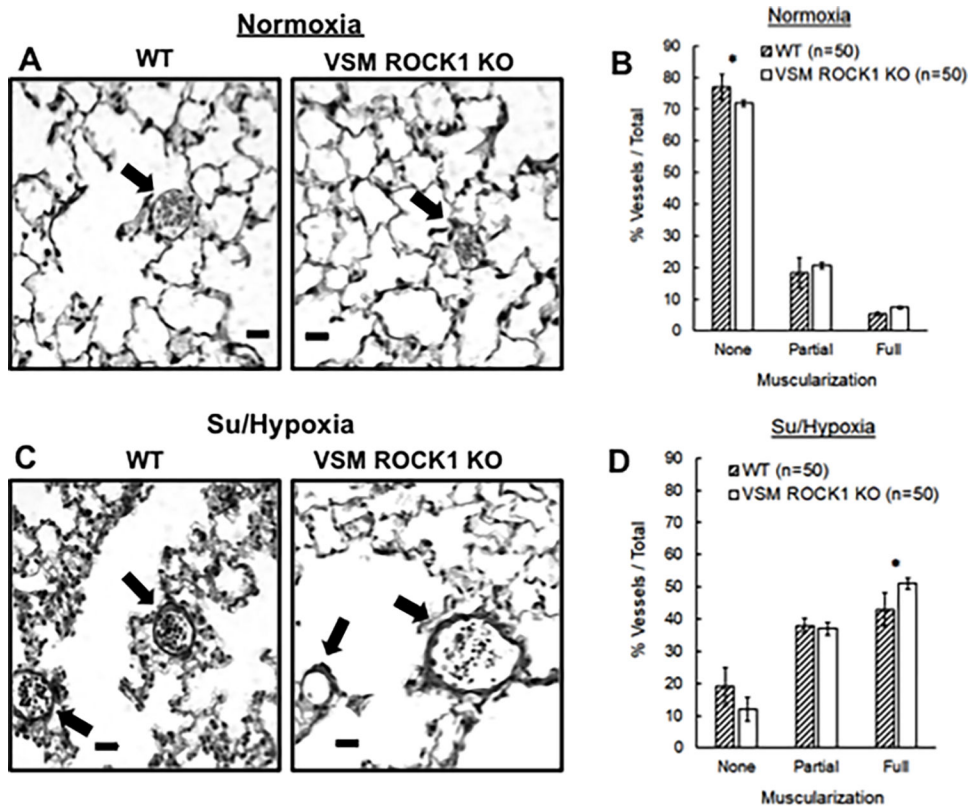
Figure 2. Morphometric analysis of small pulmonary vessels from WT and VSM ROCK1 KO animals.

Verhoeff-Van Gieson stained lung sections from A) WT or KO mice in normoxia and C) Su/Hypoxia-exposed WT and KO mice; arrows indicate small vessels; bar= 20 um. B) and D) vessels (20–80 μm diameter) were scored as none=nonmuscular, partial=partially muscular, or full=fully muscularized. Bar graphs depict values as % total small vessels; n=4 animals/group, B) *p<0.05 for non-muscularized groups vs. others in normoxia. D) *p<0.05 for fully-muscularized groups vs. others after Su/hypoxia.
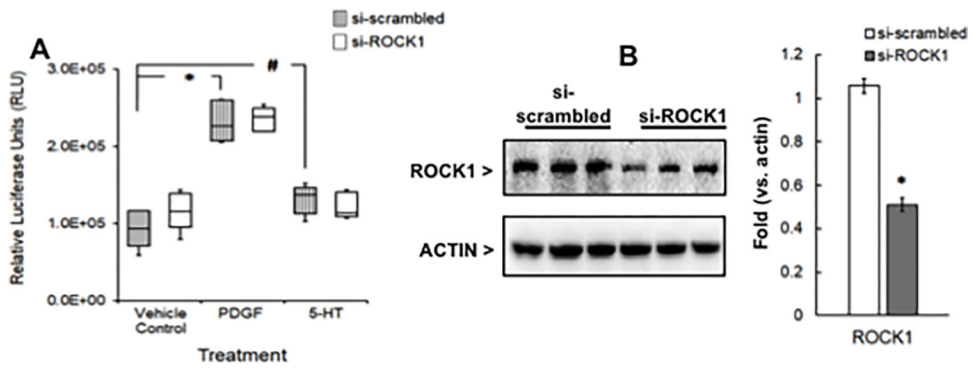
Figure 3. Effect of ROCK1 KD on growth of human PAH PASMC.

A) Scrambled (si-scrambled) or ROCK1 (si-ROCK1) siRNA-transfected cells were stimulated with vehicle, PDGF or 5-HT. Box plot depicts mean + range values from a representative experiment, n=6/group, *p<0.05 for PDGF- vs. vehicle-treated si-scr group; #p = 0.07 for 5-HT-treated vs. vehicle-treated si-scr group. B) Lysates of siRNA-transfected PAH PASMC immunoblotted for ROCK1 and actin; bar graph depicts mean fold ROCK1 levels normalized to actin levels; *p<0.05.
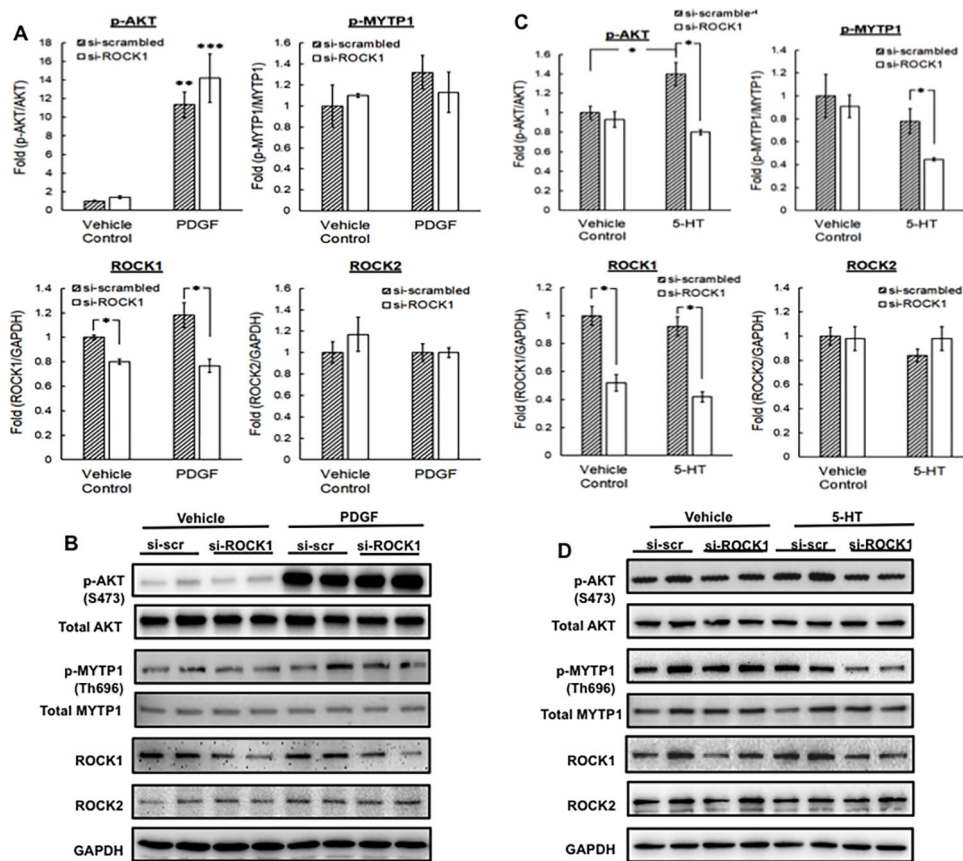
Figure 4. Effect of ROCK1 KD on signaling in human PAH-PASMC.
(**A and B**) si-Scr or si-ROCK1-transfected cells were stimulated with PDGF and lysates immunoblotted as designated. A) Bar graphs depict fold mean $\pm$ SEM densitometric values of bands calculated by assigning a value of 1 to the vehicle-treated si-scr mean. **$p<0.05$ for si-scr+PDGF p-AKT vs. +vehicle group: ***$p<0.05$ for p-AKT si-ROCK1+PDGF p-AKT vs. +vehicle group. *$p<0.05$ for differences in ROCK1 fold-mean between si-ROCK1 and si-scr groups. B) Panels show representative immunoblots of vehicle and PDGF-treated lysates with duplicate samples. (**C and D**) si-Scr or si-ROCK1-transfected cells were stimulated with 5-HT and lysates immunoblotted as designated. C) Bar graphs depict fold mean $\pm$ SEM densitometric values of bands after normalization as in A) above; *$p<0.05$ for differences in fold-mean p-AKT and p-MYPT1 groups as designated. D) Panels show representative immunoblots of vehicle and 5-HT-treated lysates with duplicate samples.